A New Adaptive Sliding-Mode Control Scheme for Application to Robot Manipulators

Jaemin Baek, *Student Member, IEEE*, Maolin Jin, *Member, IEEE*, and Soohee Han, *Senior Member, IEEE*

Abstract—This paper presents a new adaptive sliding-mode control (ASMC) scheme that uses the time-delay estimation (TDE) technique, then applies the scheme to robot manipulators. The proposed ASMC uses a new adaptive law to achieve good tracking performance with small chattering effect. The new adaptive law considers an arbitrarily small vicinity of the sliding manifold, in which the derivatives of the adaptive gains are inversely proportional to the sliding variables. Such an adaptive law provides remarkably fast adaptation and chattering reduction near the sliding manifold. To yield the desirable closed-loop poles and simplify a complicated system model by adapting feedback compensation, the proposed ASMC scheme works together with a pole-placement control (PPC) and a TDE technique. It is shown that the tracking errors of the proposed ASMC scheme are guaranteed to be uniformly ultimately bounded (UUB) with arbitrarily small bound. The practical effectiveness and the fast adaptation of the proposed ASMC are illustrated in simulations and experiments with robot manipulators, and compared with those of an existing ASMC.

Index Terms—Adaptive sliding-mode control (ASMC), fast adaptation, robot manipulators, time-delay estimation.

I. INTRODUCTION

ROBOT manipulators help human workers perform complicated and repetitive tasks quickly and efficiently in a variety of industrial processes such as assembling [1], assisting [2], transportation [3], drilling [4], and deburring [5]. To perform such demanding and time-consuming tasks, recent robot manipulators are required to follow the desired paths more closely and have faster convergence to them [6], [7].

Generally, motion control of robot manipulators is a difficult task because of high nonlinearity, coupling dynamics effects, time-varying parameters, unknown disturbances, and modeling uncertainties. Such undesirable factors may result in inaccu-

rate motion of joints of robot manipulators and finally lead to their instability. To solve these problems, various robust control algorithms have been developed, including sliding-mode control (SMC) [8], [9], time-delay control [10], [11], neural networks [12], [13], and finite-time control [14], [15].

As one of representative robust nonlinear control schemes, SMC is well established, simple, and widely applicable [16], [17]. The outstanding feature of SMC is its robustness to unknown system dynamics. If the switching gains of SMC are chosen to be greater than the upper bound on the uncertain or unmodeled terms, robust stabilization is ideally achieved. In reality, however, the upper bound is unknown , so the switching gains are chosen to be large enough to cover a wide range of uncertainties. Such large switching gains may cause chattering, in which the robot manipulator oscillates around the sliding manifold because of physical imperfections in switching devices and the time delays that often occur in real systems [18], [19]. Chattering results in serious problems such as high heat losses in electrical power circuits and high wear of moving mechanical parts. Such chattering arising in SMC has challenged ones to develop more effective control methods to suppress them and then to satisfy given control objectives in a more systematic way. These methods include the boundary layer setting [20], [21], low-pass filtering [22], [23], and higher order control [24], [25]. However, these approaches still have the limitation that they require information about the upper bound on the uncertain terms. For this reason, adaptive sliding-mode control (ASMC) has been developed to provide more fundamental remedies for chattering problems, whose adaptive switching gains are adjusted regardless of the upper bound on the uncertain terms.

Some approaches have been used to design ASMCs that do not require knowledge of the upper bound on the uncertain terms. ASMCs have been developed for use when upper bounds are unknown and unstructured [26], [27]. These ASMCs may provide conservative results since they consider the unstructured upper bounds. Furthermore, chattering still happens due to monotonically increasing switching gains for guaranteeing the asymptotic stability [26] and the slow adaptation speed near the sliding manifold from slow-varying switching gains [27]. As another approach, ASMCs with parameterized upper bounds were proposed in consideration of unknown and structured upper bounds to reduce the conservatism of results [28], [29]. These ASMCs also have the possibility of chattering because of nondecreasing switching gains. Especially in [29], the concept of the boundary layer has been applied to reduce chattering, but this method may result in poor tracking performance since the effort to reduce chattering degrades the

tracking ability [30]. To the best of authors' knowledge, there is no result on ASMCs that are designed for achieving both good tracking performance and chattering reduction simultaneously. It would be practical and meaningful to develop a new version of ASMCs that provides good tracking performance, chattering reduction, and simple structure for implementation without using the knowledge of the upper bounds on uncertain terms.

In this paper, we propose a new model-free and simple ASMC scheme with fast adaptation and powerful abilities for tracking and chattering reduction. The adaptive law of the proposed ASMC guarantees that within a finite time, the sliding variables enter an arbitrarily small vicinity of the sliding manifold and then stay around it. To achieve fast adaptation or fast convergence to the sliding manifold, the derivatives of the switching gains are proportional to the sliding variables away from the sliding manifold. On the other hand, once the sliding variables become close to the sliding manifold, the derivatives of the switching gains are inversely proportional to them in order to reduce chattering. Even though switching gains become somewhat large to achieve good tracking performance and robustness, chattering is not much influenced, because the adaptation speed is fast. For these reasons, the adaptive law of the proposed ASMC attains good tracking performance with small chattering effect. To obtain the desired error dynamics and cancel out uncertainties by feedback compensation, the proposed ASMC works together with a pole-placement control (PPC) and time-delay estimation (TDE) technique [31]–[36]. The TDE technique provides a simple system model by canceling out uncertainties, nonlinearities, and disturbances arising in real systems. Hence, this technique enables increasing the effectiveness with which control schemes can be designed. However, the TDE technique causes the so-called TDE errors because the estimation is delayed by one sampling step. Fortunately, these errors are known to be bounded [37] and are shown in this paper to be suppressed by the proposed ASMC. It is ascertained that the auxiliary PPC and TDE technique help improving the performance of the proposed ASMC. It is shown that the tracking errors of the proposed ASMC scheme, combined with PPC and TDE technique, are guaranteed to be uniformly ultimately bounded (UUB) with an arbitrarily small bound by using a Lyapunov approach. The practical feasibility and the fast adaptation of the proposed ASMC are illustrated in simulations and experiments with a robot manipulator, and compared with those of an existing ASMC [27].

This paper is organized as follows. In Section II, we develop a new version of ASMC for a robot manipulator. In Section III, simulations of a two-link robot manipulator are presented. In Section IV, the proposed ASMC scheme is applied to a real robot manipulator. In Section V, we conclude with a brief summary of this paper.

II. NEW ADAPTIVE SLIDING-MODE CONTROL SCHEME

The dynamics of a general robot manipulator [38] in n-degree of freedom (DOF) can be described as

$$\boldsymbol{\tau}(t) = \mathbf{M}(\mathbf{q}(t))\ddot{\mathbf{q}}(t) + \mathbf{C}(\mathbf{q}(t),\dot{\mathbf{q}}(t))\dot{\mathbf{q}}(t)$$
$$+ \mathbf{g}(\mathbf{q}(t)) + \mathbf{f}(\dot{\mathbf{q}}(t)) \tag{1}$$

where $\mathbf{q}(t) \in \Re^n, \dot{\mathbf{q}}(t) \in \Re^n$, and $\ddot{\mathbf{q}}(t) \in \Re^n$ are the angle, the angular velocity, and the angular acceleration of the joints, respectively, $\boldsymbol{\tau}(t) \in \Re^n$ is the control input torque, $\mathbf{M}(\mathbf{q}(t)) \in \Re^{n \times n}$ is the symmetric positive definite inertia matrix, $\mathbf{C}(\mathbf{q}(t),\dot{\mathbf{q}}(t)) \in \Re^n$ is the Coriolis matrix, $\mathbf{g}(\mathbf{q}(t)) \in \Re^n$ is the gravity force, and $\mathbf{f}(\dot{\mathbf{q}}(t)) \in \Re^n$ is the friction force.

Multiplying both sides of (1) by $\mathbf{M}^{-1}(\mathbf{q}(t))$ and solving for $\ddot{\mathbf{q}}(t)$, we have

$$\ddot{\mathbf{q}}(t) = -\mathbf{M}^{-1}(\mathbf{q}(t))\{\mathbf{C}(\mathbf{q}(t),\dot{\mathbf{q}}(t))\dot{\mathbf{q}}(t) + \mathbf{g}(\mathbf{q}(t))\}$$
$$- \mathbf{M}^{-1}(\mathbf{q}(t))\mathbf{f}(\dot{\mathbf{q}}(t)) + \{\mathbf{M}^{-1}(\mathbf{q}(t)) - \bar{\mathbf{M}}^{-1}\}\boldsymbol{\tau}(t)$$
$$+ \bar{\mathbf{M}}^{-1}\boldsymbol{\tau}(t) \tag{2}$$

where $\bar{\mathbf{M}} = \mathrm{diag}(\bar{m}_1, \bar{m}_2, \ldots, \bar{m}_n) \in \Re^{n \times n}$ is a constant matrix to be determined later on for guaranteeing the stability. Representing (2) in a compact and simple form yields

$$\ddot{\mathbf{q}}(t) = \boldsymbol{\Gamma}(t) + \bar{\mathbf{M}}^{-1}\boldsymbol{\tau}(t) \tag{3}$$

where $\boldsymbol{\Gamma}(t) = -\mathbf{M}^{-1}(\mathbf{q}(t))\{\mathbf{C}(\mathbf{q}(t),\dot{\mathbf{q}}(t))\dot{\mathbf{q}}(t) + \mathbf{g}(\mathbf{q}(t))\} - \mathbf{M}^{-1}(\mathbf{q}(t))\mathbf{f}(\dot{\mathbf{q}}(t)) + \{\mathbf{M}^{-1}(\mathbf{q}(t)) - \bar{\mathbf{M}}^{-1}\}\boldsymbol{\tau}(t) \in \Re^n$ includes all remaining terms except the last term in (2). In this paper, we make the well-known and acceptable assumption that the robotic dynamics in (1) satisfies $||\mathbf{M}^{-1}(\mathbf{q}(t))||_2 \le \delta_M$ for a positive constant δ_M.

The control objective in this paper is to make the joint angles of a robot manipulator $\mathbf{q}(t)$ follow the reference $\mathbf{q}_d(t)$ precisely, which means that the tracking error $\mathbf{e}(t) = \mathbf{q}_d(t) - \mathbf{q}(t)$ is suppressed as much as possible. To achieve such a control objective, we shall first define the following sliding variable:

$$\mathbf{s}(t) = \dot{\mathbf{e}}(t) + \mathbf{K}_s\mathbf{e}(t) \tag{4}$$

where $\mathbf{s}(t) = [s_1(t), s_2(t), \ldots, s_n(t)]^T \in \Re^n$ and $\mathbf{K}_s = \mathrm{diag}(k_{s1}, \ldots, k_{sn}) \in \Re^{n \times n}$. It is noted that $\mathbf{K}_s$ in (4) is a design parameter to be determined for guaranteeing the stability. In terms of the sliding variable $\mathbf{s}(t)$ in (4), we construct the following control [39]:

$$\bar{\boldsymbol{\tau}}(t) = -\bar{\mathbf{M}}\hat{\boldsymbol{\Gamma}}(t) + \bar{\mathbf{M}}\left(\ddot{\mathbf{q}}_d(t) + \mathbf{K}_s\dot{\mathbf{e}}(t) + \beta\mathbf{s}(t)\right) \tag{5}$$

where $\beta \in \Re$ is a positive scalar-design parameter. It is noted that $\bar{\boldsymbol{\tau}}(t)$ in (5) is distinguished from the real control input $\boldsymbol{\tau}(t)$ in (1) that will be determined by providing an additional control input term to $\bar{\boldsymbol{\tau}}(t)$. $\hat{\boldsymbol{\Gamma}}(t)$ is an estimate of $\boldsymbol{\Gamma}(t)$ in (3), and it can be obtained from one sample-delayed measurement of $\boldsymbol{\Gamma}(t)$, which is called the TDE technique. In other words, we have

$$\hat{\boldsymbol{\Gamma}}(t) = \boldsymbol{\Gamma}(t-L) = \ddot{\mathbf{q}}(t-L) - \bar{\mathbf{M}}^{-1}\boldsymbol{\tau}(t-L) \tag{6}$$

where L is a sampling time period and the second equality comes from (3). Substituting (6) into (5), we have

$$\bar{\boldsymbol{\tau}}(t) = \underbrace{-\bar{\mathbf{M}}\ddot{\mathbf{q}}(t-L) + \boldsymbol{\tau}(t-L)}_{\text{TDE}}$$
$$+ \underbrace{\bar{\mathbf{M}}\left(\ddot{\mathbf{q}}_d(t) + \mathbf{K}_s\dot{\mathbf{e}}(t) + \beta\mathbf{s}(t)\right)}_{\text{PPC}} \tag{7}$$
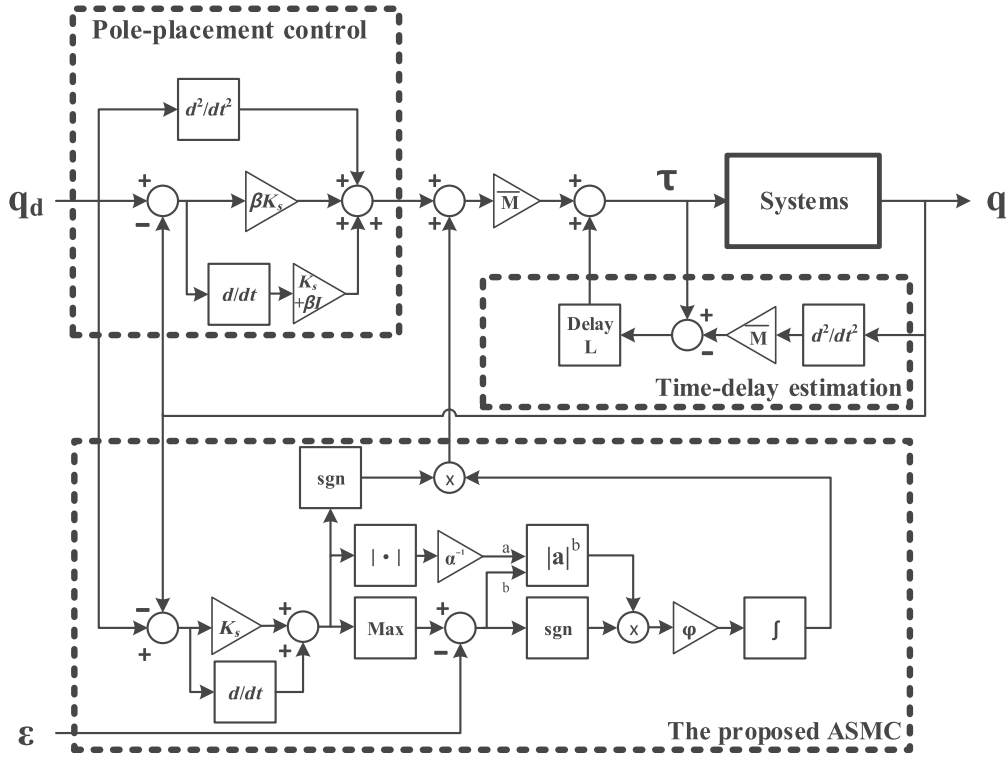
Fig. 1. Block diagram of the proposed ASMC scheme.

where $\bar{\tau}(t)$ is called a PPC scheme through this paper. Substituting the control input (7) into (3), replacing the sliding variable $\mathbf{s}(t)$ with (4), and rearranging terms yield

$$\ddot{\mathbf{e}}(t) + \mathbf{K}_d\dot{\mathbf{e}}(t) + \mathbf{K}_p\mathbf{e}(t) + \boldsymbol{\Gamma}(t) - \hat{\boldsymbol{\Gamma}}(t) = 0 \qquad (8)$$

where $\mathbf{K}_d = \mathbf{K}_s + \beta\mathbf{I} = \text{diag}(k_{d1}, k_{d2}, \ldots, k_{dn}) \in \Re^{n \times n}$ and $\mathbf{K}_p = \beta\mathbf{K}_s = \text{diag}(k_{p1}, k_{p2}, \ldots, k_{pn}) \in \Re^{n \times n}$. If we can make $\boldsymbol{\Gamma}(t) - \hat{\boldsymbol{\Gamma}}(t) = 0$, or estimate $\boldsymbol{\Gamma}(t)$ exactly, the tracking error $\mathbf{e}(t)$ in (8) goes to zero and its convergence speed can also be adjusted by choosing proper $\mathbf{K}_s$ and β to obtain desired poles. In this paper, we just choose a simple PPC to stabilize a linear system that is obtained through TDE technique. If the sampling time L is sufficiently small, the estimation in (6) implies that $\hat{\boldsymbol{\Gamma}}(t)$ can be as close to $\boldsymbol{\Gamma}(t)$ as possible. However, in reality, $\boldsymbol{\Gamma}(t)$ cannot be estimated exactly even for small sampling period L. This is because the error between $\hat{\boldsymbol{\Gamma}}(t)$ and $\boldsymbol{\Gamma}(t)$, called TDE errors, is inevitable due to inherent measurement noises and hard nonlinearity as well as to a limited sampling period [40]. It is necessary to suppress such TDE errors by using a special control algorithm. We propose a new version of ASMC and add it to the control in (7) as follows:

$$\boldsymbol{\tau}(t) = \underbrace{-\bar{\mathbf{M}}\ddot{\mathbf{q}}(t - L) + \boldsymbol{\tau}(t - L)}_{\text{TDE}}$$
$$+ \underbrace{\bar{\mathbf{M}}\left(\ddot{\mathbf{q}}_d(t) + \mathbf{K}_s\dot{\mathbf{e}}(t) + \beta\mathbf{s}(t)\right)}_{\text{PPC}}$$
$$+ \underbrace{\bar{\mathbf{M}}\left(\hat{\mathbf{K}}(t) \cdot \text{sgn}(\mathbf{s}(t))\right)}_{\text{The proposed ASMC}} \qquad (9)$$

where $\hat{\mathbf{K}}(t) = \text{diag}(\hat{k}_1(t), \hat{k}_2(t), \ldots, \hat{k}_n(t)) \in \Re^{n \times n}$ are positive switching gains to be determined for guaranteeing stability, and the proposed ASMC scheme (9) is the PPC scheme (7) when the switching gains $\hat{\mathbf{K}}(t)$ are set to be zero. It is noted that we do not apply any approximation to the computation of the signum function $\text{sgn}(\mathbf{s}(t)) = [\text{sgn}(s_1(t)), \text{sgn}(s_2(t)), \ldots, \text{sgn}(s_n(t))]^T \in \Re^n$ defined by

$$\text{sgn}(s_i(t)) = \begin{cases} 1, & \text{if } s_i(t) \geq 0 \\ -1, & \text{if } s_i(t) < 0. \end{cases} \qquad (10)$$

The proposed ASMC scheme in (9) can be depicted with a block diagram as seen in Fig. 1. The proposed ASMC employs a new adaptive law as follows:

$$\dot{\hat{k}}_i(t) = \begin{cases} \varphi_i \cdot \left\{\alpha_i^{-1} \cdot |s_i(t)|\right\}^{\theta(t)} \cdot \theta(t), & \text{if } \hat{k}_i(t) > 0 \\ \varphi_i \cdot \alpha_i^{-1} \cdot |s_i(t)|, & \text{if } \hat{k}_i(t) = 0 \end{cases} \qquad (11)$$

where φ_i and α_i are tunable positive gains for adaptation speed and $\theta(t)$ is defined as $\text{sgn}(\|\mathbf{s}(t)\|_\infty - \varepsilon)$ with a positive-design parameter ε. The adaptation speed of switching gains $\hat{k}_i(t)$ is highly affected by ε.

As seen in (11), the proposed adaptive law does not require the information on the upper bound of uncertain and unmodeled terms. For $\hat{k}_i(t) > 0$, the adaptive law has two different forms according to the output of the signum function: $\|\mathbf{s}(t)\|_\infty \geq \varepsilon$ and $\|\mathbf{s}(t)\|_\infty < \varepsilon$. When $\|\mathbf{s}(t)\|_\infty \geq \varepsilon$, the switching gain $\hat{k}_i(t)$ increases until $\|\mathbf{s}(t)\|_\infty < \varepsilon$. As the switching gains $\hat{k}_i(t)$ are more and more increasing, the sliding variable $\mathbf{s}(t)$ goes to the vicinity of the sliding manifold more quickly. Once the sliding variable enters the vicinity of the sliding manifold,

i.e., $||\mathbf{s}(t)||_\infty < \varepsilon$, the switching gain $\hat{k}_i(t)$ decreases while the sliding variable stays in the vicinity of the sliding manifold. Furthermore, such decreasing speed of the switching gains becomes fast and then the corresponding adaptation speed also increases, because the proposed adaptive law (11) is inversely proportional to the sliding variable when $||\mathbf{s}(t)||_\infty < \varepsilon$. For this reason, even though the switching gains keep high temporarily for a small ε, the proposed adaptive law reduces chattering. The proposed adaptive law can be said to provide better tracking performance and chattering reduction simultaneously due to its high switching gains and fast adaptation speed. Before showing the UUB property of the proposed adaptive law (11), we introduce two Lemmas that will be helpful in the proof of the main results.

Lemma 1: [37] If the control gain $\bar{\mathbf{M}}$ in (9) is chosen to satisfy the following condition:

$$||\mathbf{I} - \mathbf{M}^{-1}(\mathbf{q}(t))\,\bar{\mathbf{M}}||_2 < 1$$

for all $t \geq 0$, then $||\ddot{\mathbf{q}}(t - L) - \ddot{\mathbf{q}}(t)||_2 \to 0$ as $L \to 0$ and the TDE errors are bounded by constant Γ_i^* for all $i = 1, 2, \ldots, n$, i.e., $|\Gamma_i(t) - \hat{\Gamma}_i(t)| \leq \Gamma_i^*$.

Lemma 2: For a robot manipulator (1) controlled by (9) and (11), the switching gain $\hat{k}_i(t)$ is upper bounded by a positive constant $\hat{k}_i^*$ as follows:

$$\hat{k}_i(t) < \hat{k}_i^*$$

for $t \geq 0$.

Proof: The proof is given in Appendix. ∎

Theorem 1: For a robot manipulator (3) controlled by (9) and (11), the sliding variables enter the vicinity of the sliding manifold, $||\mathbf{s}(t)||_\infty < \varepsilon$, within a finite time $t_\varepsilon > 0$, and then they are guaranteed to be UUB for $t \geq t_\varepsilon$ as follows:

$$||\mathbf{s}(t)||_2 < \sqrt{\sum_{i=1}^n \varepsilon^2 + \tilde{k}_M}$$

where $\tilde{k}_M$ is the maximum value of $\sum_{i=1}^n \frac{\alpha_i}{\varphi_i}\left(\Gamma_i^* - \hat{k}_i(t)\right)^2$.

Proof: We choose a Lyapunov function as

$$V(t) = \frac{1}{2}\mathbf{s}^T(t)\mathbf{s}(t) + \frac{1}{2}\sum_{i=1}^n \frac{\alpha_i}{\varphi_i}(\Gamma_i^* - \hat{k}_i(t))^2. \qquad (12)$$

Taking the derivative of the Lyapunov function with respect to the time t, we have

$$\dot{V}(t) = \mathbf{s}^T(t)\dot{\mathbf{s}}(t) - \sum_{i=1}^n \frac{\alpha_i}{\varphi_i}\left(\Gamma_i^* - \hat{k}_i(t)\right)\dot{\hat{k}}_i(t). \qquad (13)$$

Substituting (3) and (4) into (13) yields

$$\dot{V}(t) = \mathbf{s}^T(t)\left(-\mathbf{N}(t) - \hat{\mathbf{\Gamma}}(t) + \boldsymbol{\delta}(t)\right) - \Lambda(t) \qquad (14)$$

where $\Lambda(t)$, $\boldsymbol{\delta}(t)$, and the TDE errors $\mathbf{N}(t)$ are defined by $\sum_{i=1}^n \frac{\alpha_i}{\varphi_i}\left(\Gamma_i^* - \hat{k}_i(t)\right)\dot{\hat{k}}_i(t) \in \Re$, $-\bar{\mathbf{M}}^{-1}\boldsymbol{\tau}(t) + \ddot{\mathbf{q}}_d(t) +$

$\mathbf{K}_s\dot{\mathbf{e}}(t) \in \Re^n$, and $\mathbf{\Gamma}(t) - \hat{\mathbf{\Gamma}}(t) \in \Re^n$, respectively. Substituting (6) and (9) into (14), we have

$$\begin{aligned}\dot{V}(t) &= \sum_{i=1}^n s_i(t)\left(-N_i(t) - \beta s_i(t) - \hat{k}_i(t)\mathrm{sgn}(s_i(t))\right) - \Lambda(t)\\ &\leq \sum_{i=1}^n |s_i(t)||N_i(t)| - \sum_{i=1}^n |s_i(t)|\hat{k}_i(t)\\ &\quad - \beta\sum_{i=1}^n s_i^2(t) - \Lambda(t)\\ &= \sum_{i=1}^n \left(|s_i(t)| - \frac{\alpha_i}{\varphi_i}\dot{\hat{k}}_i(t)\right)\left(\Gamma_i^* - \hat{k}_i(t)\right) - \beta\cdot\sum_{i=1}^n s_i^2(t)\end{aligned}$$

$$(15)$$

where $\mathbf{N}(t) = [N_1(t), N_2(t), \ldots, N_n(t)]^T \in \Re^n$ and the second equality comes from the proposed adaptive law (11). We consider two cases: $||\mathbf{s}(t)||_\infty \geq \varepsilon$ and $||\mathbf{s}(t)||_\infty < \varepsilon$. In the case of $||\mathbf{s}(t)||_\infty \geq \varepsilon$, it follows from (15) that we have

$$\dot{V}(t) \leq -\beta\sum_{i=1}^n s_i^2(t). \qquad (16)$$

The inequality (16) means that $V(t)$ is decreasing and bounded since $0 \leq V(t) \leq V(0) < \infty$. From (16), we also have

$$\dot{V}(t) \leq -\beta\sum_{i=1}^n s_i^2(t) \leq -\beta\varepsilon^2 \qquad (17)$$

which means that the sliding variable $\mathbf{s}(t)$ arrives at the small vicinity of the sliding manifold, i.e., $||\mathbf{s}(t)||_\infty < \varepsilon$ within a finite time $t_\varepsilon > 0$.

Even though within a finite time, the sliding variable $\mathbf{s}(t)$ enters the region $||\mathbf{s}(t)||_\infty < \varepsilon$, it may move in and out since $\dot{V}(t)$ is not guaranteed to be nonpositive in this vicinity of the sliding manifold. If the sliding variable $\mathbf{s}(t)$ leaves the region $||\mathbf{s}(t)||_\infty < \varepsilon$, $\dot{V}(t)$ becomes negative again according to (16), which steers it back toward the sliding manifold.

Now, we shall obtain the upper bound of $||\mathbf{s}(t)||_2$, which will be valid since the first time when the sliding variable $\mathbf{s}(t)$ enters the region $||\mathbf{s}(t)||_\infty < \varepsilon$. To begin with, it can be seen in (12) that the Lyapunov function $V(t)$ is bounded as

$$\frac{1}{2}||\mathbf{s}(t)||_2^2 \leq V(t) \leq \frac{1}{2}||\mathbf{s}(t)||_2^2 + \frac{1}{2}\sum_{i=1}^n \frac{\alpha_i}{\varphi_i}\left(\Gamma_i^* - \hat{k}_i(t)\right)^2. \qquad (18)$$

It is noted that $\frac{1}{2}\sum_{i=1}^n \frac{\alpha_i}{\varphi_i}\cdot\left(\Gamma_i^* - \hat{k}_i(t)\right)^2$ in (18) is bounded because Γ_i^* is constant and $\hat{k}_i(t)$ is bounded according to Lemma 2. It follows then that we have

$$V(t) < \frac{1}{2}\sum_{i=1}^n \varepsilon^2 + \frac{1}{2}\sum_{i=1}^n \tilde{k}_M. \qquad (19)$$

Putting (18) and (19) together yields

$$\frac{1}{2}||\mathbf{s}(t)||_2^2 < \frac{1}{2}\sum_{i=1}^n \varepsilon^2 + \frac{1}{2}\tilde{k}_M \qquad (20)$$

which means that

$$||\mathbf{s}(t)||_2 < \sqrt{\sum_{i=1}^n \varepsilon^2 + \tilde{k}_M}. \qquad (21)$$

Equation (21) implies that the sliding variable $\mathbf{s}(t)$ is UUB for $t \geq t_\varepsilon$. Although the sliding variable $\mathbf{s}(t)$ moves in and out of the small vicinity of the sliding manifold due to the attractivity from (16), it is guaranteed to be upper-bounded by (21). The upper bound in (21) can be adjusted by parameters φ_i, α_i, and ε. ∎

According to Theorem 1, $||\mathbf{s}(t)||_2$ is upper-bounded and serves as a bounded input for a dynamic system (4). Since $\dot{\mathbf{e}}(t) = -\mathbf{K}_s\mathbf{e}(t)$ in (4) is asymptotically stable and $\mathbf{s}(t)$ is bounded, the tracking error $\mathbf{e}(t)$ is also bounded, which means bounded input and bounded output (BIBO) stability [41].

III. SIMULATION

A. Simulation Setup

To illustrate the performance of the proposed ASMC scheme, we conducted simulations with a two-link robot manipulator depicted in Fig. 2. Its dynamics [42] is given as

$$\mathbf{M}(\mathbf{q})$$
$$= \begin{bmatrix} l_2^2 m_2 + 2l_1 l_2 m_2 c_2 + l_1^2(m_1 + m_2) & l_2^2 m_2 + l_1 l_2 m_2 c_2 \\ l_2^2 m_2 + l_1 l_2 m_2 c_2 & l_2^2 m_2 \end{bmatrix}$$

$$\mathbf{C}(\mathbf{q}, \dot{\mathbf{q}})\dot{\mathbf{q}} = \begin{bmatrix} -m_2 l_1 l_2 s_2 \dot{q}_2^2 - 2m_2 l_1 l_2 s_2 \dot{q}_1 \dot{q}_2 \\ m_2 l_1 l_2 s_2 \dot{q}_2^2 \end{bmatrix}$$

$$\mathbf{G}(\mathbf{q}) = \begin{bmatrix} m_2 l_2 g c_{12} + (m_1 + m_2) l_1 g c_1 \\ m_2 l_2 g c_{12} \end{bmatrix}$$

$$\mathbf{F}(\dot{\mathbf{q}}) = \begin{bmatrix} \alpha_1 \cdot \mathrm{sgn}(\dot{q}_1) \\ \alpha_2 \cdot \mathrm{sgn}(\dot{q}_2) \end{bmatrix}$$

where q_i is the angle for the joint i, and s_i, c_i, and c_{ij} are defined by $\sin(q_i(t))$, $\cos(q_i(t))$, and $\cos(q_i(t) + q_j(t))$, respectively. The lengths of the links are set to be $l_1 = 0.2$ m and $l_2 = 0.1$ m, the gravitational acceleration to be $g = 9.81$ m/s², the friction coefficient to be $\alpha_1 = \alpha_2 = 50$, and the end tip loads of the joints 1 and 2 to be $m_1 = 10$ kg and $m_2 = 5$ kg, respectively. The control objective is to make the angles of the joints 1 and 2 follow the desired reference trajectories well. We choose the desired trajectories as in Figs. 3 and 4. In Fig. 4, it is only used to confirm the tracking errors.

B. Simulation Results

The practical efficiency and the fast adaptation speed of the proposed ASMC are shown through simulations and comparisons with the existing ASMC [27] and the boundary layer-based SMC control (BSMC) [43]. For fairness, all controls for
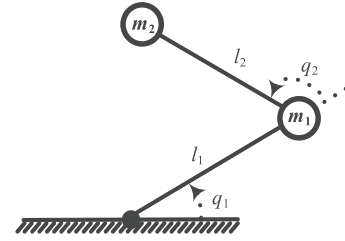

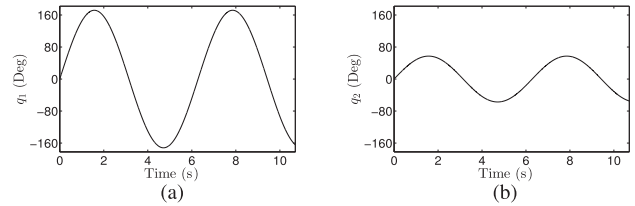
Fig. 2. Two-link robot manipulator.

Fig. 3. Trajectories of the desired smooth reference angles. (a) Joint 1. (b) Joint 2.
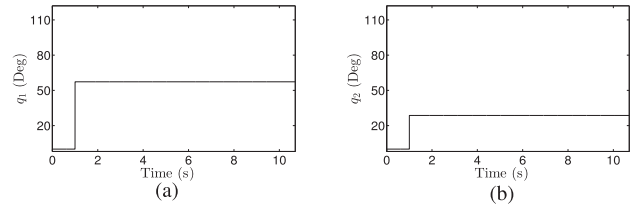

Fig. 4. Trajectories of the desired step reference angles. (a) Joint 1. (b) Joint 2.

comparison use the PPC scheme (7) as in the proposed ASMC scheme of Fig. 1. The existing ASMC combined with the PPC scheme is called "existing ASMC scheme," and BSMC combined with the PPC scheme is called "BSMC scheme" through this paper.
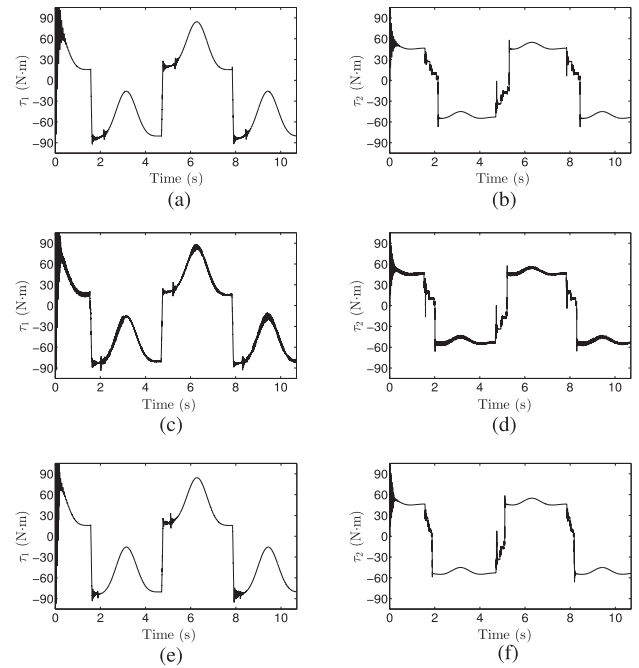
The control gain $\bar{\mathbf{M}}$ is chosen to be $\mathrm{diag}(0.01, 0.01)$ so that Lemma 1 is satisfied. Actually, $||\mathbf{I} - \mathbf{M}^{-1}(\mathbf{q}(t))\bar{\mathbf{M}}||_2$ is computed to be between 0.9869 and 0.9886. The gain $\mathbf{K}_s$, the positive constant β, and the sampling period L are taken to be $\mathrm{diag}(1, 1)$, 1, and 1 ms, respectively. The additional parameters for the proposed adaptive law (11) are given as $\varphi_1 = 4000$, $\varphi_2 = 3000$, $\alpha_1 = 0.60$, $\alpha_2 = 1.57$, and $\varepsilon = 0.015$.

Fig. 5(a), (d), and (e) shows the switching gains computed by the existing and proposed ASMC schemes. The proposed ASMC scheme involves two independent switching gains for the joints 1 and 2, while the existing one does the same switching gain for the joints 1 and 2. This use of the same switching gain means that controllers for the joints 1 and 2 share the same logic in general and that freedom of design for controls is restricted. It is observed from Fig. 5 that, when the sliding variables move out of the vicinity of sliding manifold, i.e., $||\mathbf{s}(t)||_\infty \geq \varepsilon$, the switching gains increase until the sliding variable approaches the region $||\mathbf{s}(t)||_\infty < \varepsilon$. On the other hand, the switching gains decrease when the sliding variables stay at the vicinity of sliding manifold, i.e., $||\mathbf{s}(t)||_\infty < \varepsilon$. Lemma 2 tells us that such switching gains do not diverge and have upper bounds.
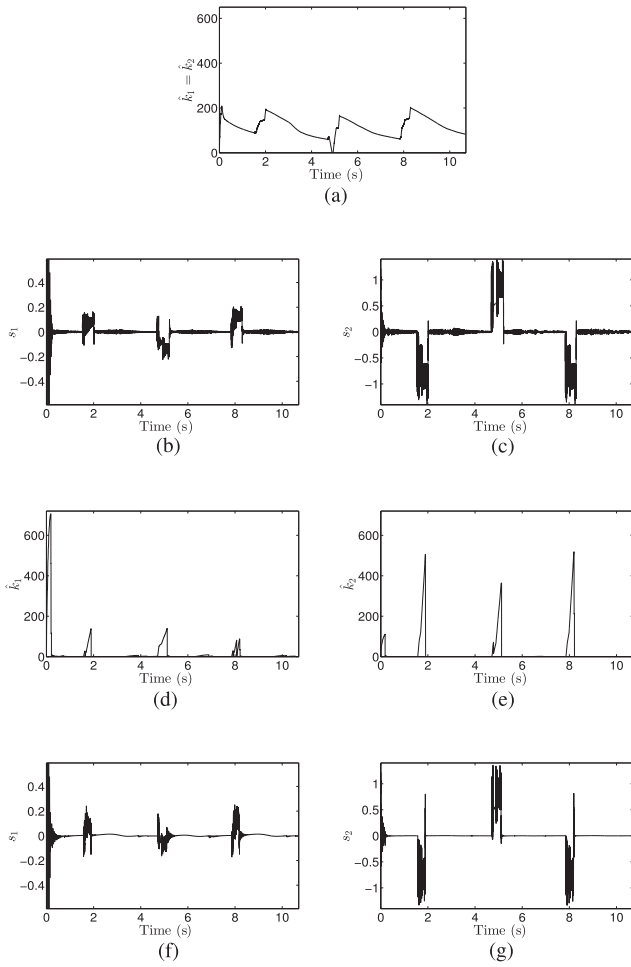
Fig. 5. Comparison of the switching gains and sliding variables generated by two controls. (a) Switching gain of the existing ASMC scheme. (b) Sliding variable of the existing ASMC scheme for the joint 1. (c) Sliding variable of the existing ASMC scheme for the joint 2. (d) Switching gain of the proposed ASMC scheme for the joint 1. (e) Switching gain of the proposed ASMC scheme for the joint 2. (f) Sliding variable of the proposed ASMC scheme for the joint 1. (g) Sliding variable of the proposed ASMC scheme for the joint 2.

Fig. 6. Comparison of the control inputs. (a) PPC scheme for the joint 1. (b) PPC scheme for the joint 2. (c) Existing ASMC scheme for the joint 1. (d) Existing ASMC scheme for the joint 2. (e) Proposed ASMC scheme for the joint 1. (f) Proposed ASMC scheme for the joint 2.

Fig. 7. Comparison of the tracking errors for smooth reference angles of the PPC scheme (dashed line), the BSMC scheme (dashed dotted line), the existing ASMC scheme (dotted line), and the proposed ASMC scheme (solid line). (a) Joint 1. (b) Joint 2.

Parameter ε in the adaptive law (11) has a critical role in the tradeoff between tracking ability and chattering reduction. If ε is too small, the existing ASMC scheme has significant chattering due to the slow adaptation speed. On the contrary, if ε is too large, the existing ASMC scheme suffers from poor tracking performance. However, the proposed ASMC scheme has fast adaptation speed of the switching gains according to (11), so it permits more freedom for selecting ε. Even though the proposed ASMC scheme applies large switching gains to achieve good tracking performance and robustness, chattering is not affected much because the large switching gains can be reduced rapidly according to (11). In addition, the trajectories of the sliding variables can be seen in Fig. 5(b), (c), (f), and (g). When the sliding variables leave the vicinity of sliding manifold, the y are strongly influenced by the switching gains. Thus, the sliding variables generated by the proposed ASMC ha ve less chattering, which is in accordance with Fig. 6. This reduction in chattering results from the fast adaptation speed that is confirmed in Fig. 5(d) and (e). For this reason, the proposed
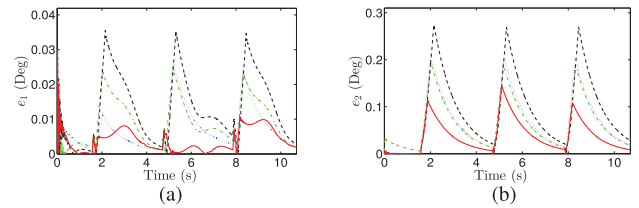
ASMC scheme provides good tracking performance with less chattering, which will be illustrated in subsequent simulations and experiments.

Fig. 6 shows the control inputs generated by the PPC scheme, the existing ASMC scheme, and the proposed ASMC scheme. The proposed ASMC scheme provides excellent chattering reduction, compared with the existing one. The control trajectory of the proposed ASMC scheme is very similar to that of the chattering-free PPC scheme.

Figs. 7 and 8 compare the tracking errors of the PPC scheme, BSMC scheme, the existing ASMC scheme, and the proposed ASMC scheme. To begin with, it can be easily seen in Figs. 7 and 8 that the BSMC scheme, the existing ASMC scheme, and proposed ASMC scheme are superior to the PPC scheme in terms of tracking errors since they have abilities to suppress TDE errors. The tracking errors of the proposed ASMC scheme are even further reduced in comparison to other controllers because the former can achieve higher switching gains than the latters while still maintaining a small chattering amplitude. Root-mean-square (rms) values of measured errors are given
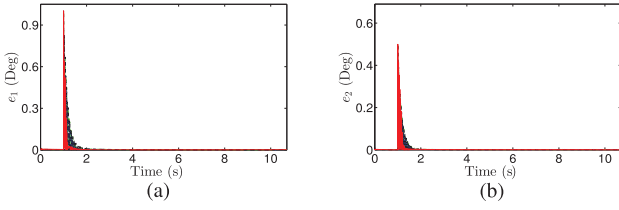
Fig. 8. Comparison of the tracking errors for step reference angles of the PPC scheme (dashed line), the BSMC scheme (dashed dotted line), the existing ASMC scheme (dotted line), and the proposed ASMC scheme (solid line). (a) Joint 1. (b) Joint 2.

TABLE I
RMS VALUES OF THE TRACKING ERRORS FOR SMOOTH REFERENCE TRAJECTORIES

Control strategies	Joint 1 (Deg)	Joint 2 (Deg)
PPC scheme	1.60×10^{-2}	11.55×10^{-2}
BSMC scheme	1.16×10^{-2}	8.11×10^{-2}
Existing ASMC scheme	0.92×10^{-2}	8.79×10^{-2}
Proposed ASMC scheme	0.50×10^{-2}	4.89×10^{-2}

TABLE II
RMS VALUES OF THE TRACKING ERRORS FOR STEP REFERENCE TRAJECTORIES (UP TO 2 S)

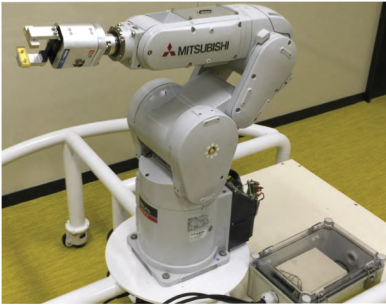| Control strategies	Joint 1 (Deg)	Joint 2 (Deg)
PPC scheme	14.70×10^{-2}	7.09×10^{-2}
BSMC scheme	14.62×10^{-2}	7.08×10^{-2}
Existing ASMC scheme	14.44×10^{-2}	7.04×10^{-2}
Proposed ASMC scheme	9.53×10^{-2}	5.44×10^{-2}

Fig. 9. MITSUBISHI RV-4FD robot manipulator.

in Tables I and II for smooth and step reference trajectories, respectively.

IV. EXPERIMENT

A. Experimental Setup

As seen in Fig. 9, a MITSUBISHI robot manipulator with two joints is used in the experiments. The maximum torque, the gear reduction ratio, and the motor encoder resolution of the joints are given as 4.5 Nm, 80:1, and 22 bits, respectively. This robot manipulator is controlled by a PC-based controller running on a real-time operating system and has a sampling period of 4 ms.

The control parameters are set to be $\beta = 20$, $\varepsilon = 35$, $\bar{\mathbf{M}} = \text{diag}(0.07, 0.12)$, $\mathbf{K}_s = \text{diag}(20, 20)$, $\alpha_1 = 300$, $\alpha_2 =$
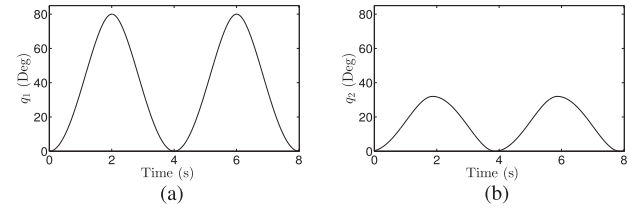

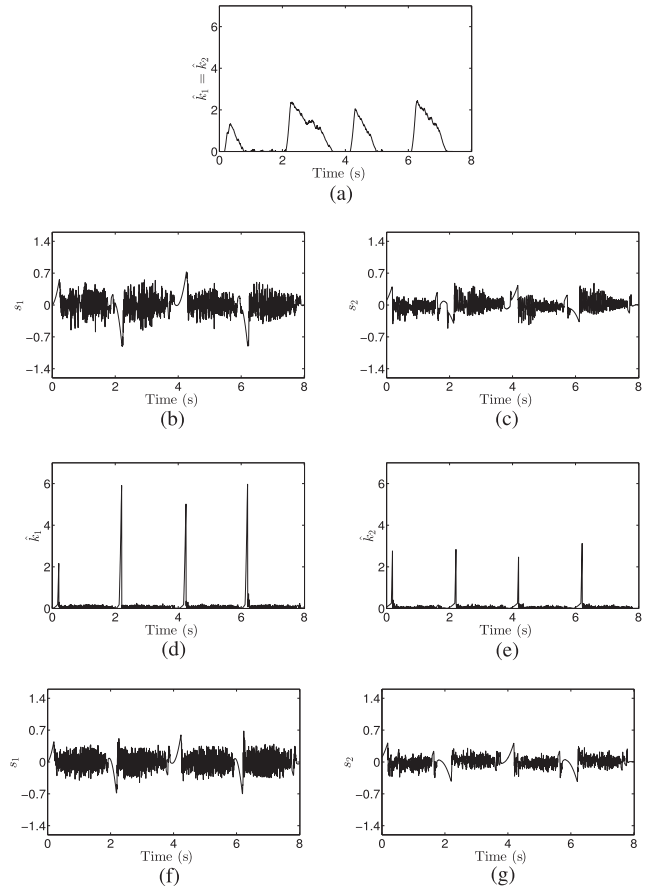Fig. 10. Trajectories of the desired reference angles. (a) Joint 1. (b) Joint 2.

Fig. 11. Comparison of the switching gains and sliding variables generated by two controls. (a) Switching gain of the existing ASMC scheme ($\times 10^3$). (b) Sliding variable of the existing ASMC scheme for the joint 1 ($\times 10^2$). (c) Sliding variable of the existing ASMC scheme for the joint 2 ($\times 10^2$). (d) Switching gain of the proposed ASMC scheme for the joint 1 ($\times 10^3$). (e) Switching gain of the proposed ASMC scheme for the joint 2 ($\times 10^3$). (f) Sliding variable of the proposed ASMC scheme for the joint 1 ($\times 10^2$). (g) Sliding variable of the proposed ASMC scheme for the joint 2 ($\times 10^2$).

200, $\varphi_1 = 4 \times 10^5$, and $\varphi_2 = 3.6 \times 10^5$. The initial conditions are chosen to be $\mathbf{q}(0) = [0, 0]$, $\dot{\mathbf{q}}(0) = [0, 0]^T$, and $\hat{\mathbf{K}}(0) = [0, 0]^T$. In other words, the robot manipulator is relaxed at $t = 0$. The trajectories for the desired angles are given as Fig. 10.

B. Experimental Results

The proposed ASMC scheme combined with the PPC scheme (7) has been verified in experiments and by comparison with the PPC scheme and the existing ASMC scheme. When we applied the proposed adaptive law (11) to a real robot manipulator, the conditions, $\hat{k}_i(t) > 0$ and $\hat{k}_i(t) = 0$, were replaced with
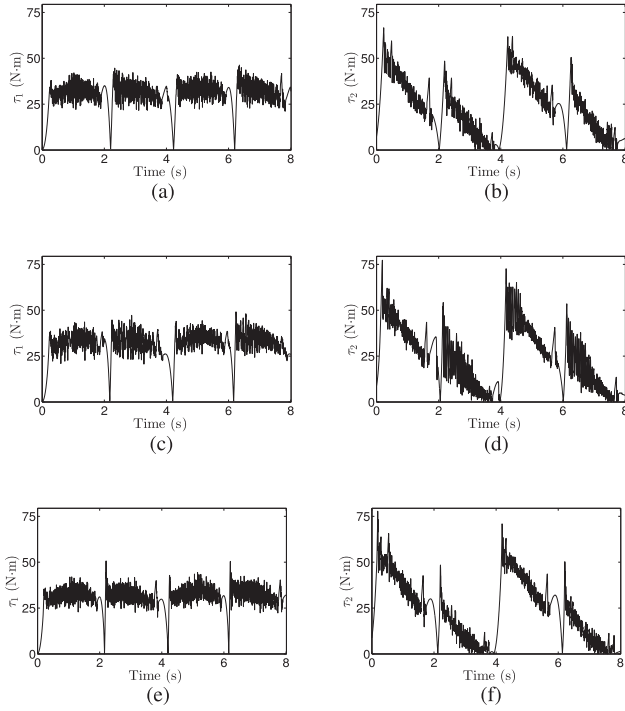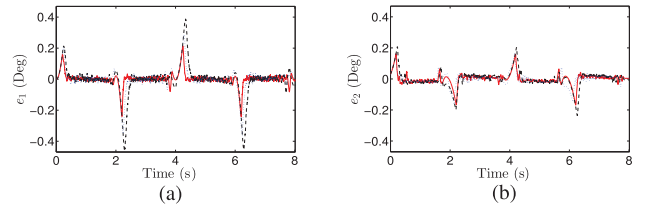
Fig. 12. Comparison of the control inputs. (a) PPC scheme for the joint 1. (b) PPC scheme for the joint 2. (c) Existing ASMC scheme for the joint 1. (d) Existing ASMC scheme for the joint 2. (e) Proposed ASMC scheme for the joint 1. (f) Proposed ASMC scheme for the joint 2.

Fig. 13. Comparison of the tracking errors generated from the PPC scheme (dashed line), the existing ASMC scheme (dotted line), and the proposed ASMC scheme (solid line). (a) Joint 1. (b) Joint 2.

TABLE III
RMS VALUES OF THE TRACKING ERRORS FOR REFERENCE TRAJECTORIES

Control strategies	Joint 1 (Deg)	Joint 2 (Deg)
PPC scheme	10.01×10^{-2}	5.39×10^{-2}
Existing ASMC scheme	7.07×10^{-2}	4.06×10^{-2}
Proposed ASMC scheme	4.32×10^{-2}	3.57×10^{-2}

$\hat{k}_i(t) > 0.0001$ and $0.0001 \geq \hat{k}_i(t) \geq 0$, respectively, to allow practical numerical computation.

Fig. 11(a), (d), and (e) shows the switching gains of the existing ASMC scheme and the proposed one. The switching gains of the proposed ASMC scheme increase or decrease depending on whether the sliding variables of the proposed ASMC scheme are close to the sliding manifold or not. Such time-varying switching gains of the proposed ASMC scheme have fast adaptation speed, and they do not diverge according to Lemma 2. In addition, the sliding variables can be seen in Fig. 11(b), (c), (f), and (g). The trajectories of the sliding variables of the proposed ASMC scheme have effects on the switching gains and are bounded according to Theorem 1.

Fig. 12 shows the control inputs obtained from the PPC scheme , the existing ASMC scheme, and the proposed ASMC scheme. It is observed that three control schemes are affected by inherent noises almost in the same degree. How much robot manipulators are affected by disturbances and noises is mostly dependent on their hardware performance. It is noted that the oscillation in Fig. 12 is basically different from chattering. In addition to such oscillation, the existing ASMC scheme suffers from chattering due to slow adaptation speed in Fig. 11(a).

Fig. 13 compares the tracking errors generated from the PPC scheme, the existing ASMC scheme, and the proposed ASMC scheme. The proposed ASMC scheme has smaller errors than the PPC scheme and the existing ASMC scheme since TDE errors are suppressed by the former and the proposed ASMC scheme has fast adaptation speed. The rms values of tracking errors are given in Table III. These results of simulations and experiments confirm the practical efficiency and fast-adaptation speed of the proposed ASMC scheme.

V. CONCLUSION

We presented a new ASMC scheme combined with the PPC and TDE technique, and applied it to robot manipulators in simulations and experiments. The proposed ASMC scheme does not require any information of the upper bounds on the uncertain or unmodeled terms, and it can provide the desirable closed-loop poles and a simple model by feedback compensation. The adaptive law employed in the proposed ASMC scheme offers remarkably fast adaptation and chattering reduction by considering an arbitrarily small vicinity of the sliding manifold. It was shown that the tracking error is guaranteed to be UUB with arbitrarily small bound while not having much effect on chattering. The proposed ASMC could be a good replacement of existing ASMC to achieve good tracking performance and reduce chattering.

APPENDIX
PROOF OF LEMMA 2

To prove Lemma 2, we need to only show that the Lyapunov function (12) is bounded. To begin with, we consider a sufficiently large number V^*. We assume that the Lyapunov function (12) has the value V^* as follows:

$$V(t) = \frac{1}{2}\mathbf{s}^T(t)\mathbf{s}(t) + \frac{1}{2}\sum_{i=1}^{n}\frac{\alpha_i}{\varphi_i}(\Gamma_i^* - \hat{k}_i(t))^2 = V^*. \quad (22)$$

Since the Lyapunov function (22) has two terms, at least one of them should be sufficiently large. If $\|\mathbf{s}(t)\|_2^2$ is sufficiently large, the derivative of the Lyapunov function (22) is negative according to (16). If the second term of the Lyapunov function (22), $\frac{1}{2}\sum_{i=1}^{n}\frac{\alpha_i}{\varphi_i}(\Gamma_i^* - \hat{k}_i(t))^2$ is sufficiently large,

the derivative of the Lyapunov function (22) can be shown to be also negative by considering the following optimization problem:

$$\max \sum_{i=1}^{n} \frac{\alpha_i}{\varphi_i} \left(\Gamma_i^* - \hat{k}_i(t) \right) \quad (23)$$

subject to

$$\frac{1}{2} \sum_{i=1}^{n} \frac{\alpha_i}{\varphi_i} (\Gamma_i^* - \hat{k}_i(t))^2 = R \le V^*, \Gamma_i \ge 0, \hat{k}_i(t) \ge 0$$

where R is a sufficiently large number less than or equal to V^*. The optimization problem in (23) clearly provides a negative optimal value since R is taken to be sufficiently large. In other words, we have

$$\sum_{i=1}^{n} \frac{\alpha_i}{\varphi_i} \cdot \left(\Gamma_i^* - \hat{k}_i(t) \right) < 0 \quad (24)$$

for a sufficiently large R. It follows then that we have

$$\dot{V}(t) \le \sum_{i=1}^{n} \left(|s_i(t)| + \frac{\alpha_i^2}{|s_i(t)|} \right) \left(\Gamma_i^* - \hat{k}_i(t) \right) - \beta \sum_{i=1}^{n} s_i^2(t).$$

In both cases where one of two terms in (22) is significantly large, $\dot{V}(t) < 0$ holds. In other words, if $V(t)$ has the value V^*, the derivative of $V(t)$ is negative. It means that $V(t)$ cannot exceed V^* and hence we have $V(t) \le V^*$. Finally, it follows that $V(t)$ is globally upper bound and $\hat{k}_i(t)$ is also upper bounded as follows:

$$\hat{k}_i(t) \le \hat{k}_i^* \quad (25)$$

for $t \ge 0$.

REFERENCES

[1] S. Chan and H. Liaw, "Generalized impedance control of robot for assembly tasks requiring compliant manipulation," *IEEE Trans. Ind. Electron.*, vol. 43, no. 4, pp. 453–461, Aug. 1996.

[2] J. Naito, G. Obinata, A. Nakayama, and K. Hase, "Development of a wearable robot for assisting carpentry workers," *Int. J. Adv. Robot. Syst.*, vol. 4, no. 4, pp. 431–436, 2007.

[3] T. Takei, R. Imamura, and S. I. Yuta, "Baggage transportation and navigation by a wheeled inverted pendulum mobile robot," *IEEE Trans. Ind. Electron.*, vol. 56, no. 10, pp. 3985–3994, Oct. 2009.

[4] W.-Y. Lee and C.-L. Shih, "Control and breakthrough detection of a three-axis robotic bone drilling system," *Mechatronics*, vol. 16, no. 2, pp. 73–84, 2006.

[5] H. Kazerooni, J. Bausch, and B. Kramer, "An approach to automated deburring by robot manipulators," *Trans. ASME, J. Dyn. Syst. Meas. Control*, vol. 108, no. 4, pp. 354–359, 1986.

[6] J. Y. Lee, M. Jin, and P. H. Chang, "Variable PID gain tuning method using backstepping control with time-delay estimation and nonlinear damping," *IEEE Trans. Ind. Electron.*, vol. 61, no. 12, pp. 6975–6985, Dec. 2014.

[7] J. Lee, P. H. Chang, and R. S. Jamisola, "Relative impedance control for dual-arm robots performing asymmetric bimanual tasks," *IEEE Trans. Ind. Electron.*, vol. 61, no. 7, pp. 3786–3796, Jul. 2014.

[8] S. Islam and P. X. Liu, "Robust sliding mode control for robot manipulators," *IEEE Trans. Ind. Electron.*, vol. 58, no. 6, pp. 2444–2453, Jun. 2011.

[9] M.-S. Park and D. Chwa, "Swing-up and stabilization control of inverted-pendulum systems via coupled sliding-mode control method," *IEEE Trans. Ind. Electron.*, vol. 56, no. 9, pp. 3541–3555, Sep. 2009.

[10] S.-J. Cho, M. Jin, T.-Y. Kuc, and J. S. Lee, "Stability guaranteed auto-tuning algorithm of a time-delay controller using a modified Nussbaum function," *Int. J. Control*, vol. 87, no. 9, pp. 1926–1935, 2014.

[11] M. Jin, S. H. Kang, and P. H. Chang, "Robust compliant motion control of robot with nonlinear friction using time-delay estimation," *IEEE Trans. Ind. Electron.*, vol. 55, no. 1, pp. 258–269, Jan. 2008.

[12] A. Abe, "Trajectory planning for flexible Cartesian robot manipulator by using artificial neural network: Numerical simulation and experimental verification," *Robotica*, vol. 29, no. 5, pp. 797–804, 2011.

[13] N. Nikdel, P. Nikdel, M. A. Badamchizadeh, and I. Hassanzadeh, "Using neural network model predictive control for controlling shape memory alloy-based manipulator," *IEEE Trans. Ind. Electron.*, vol. 61, no. 3, pp. 1394–1401, Mar. 2014.

[14] S. Yu, X. Yu, B. Shirinzadeh, and Z. Man, "Continuous finite-time control for robotic manipulators with terminal sliding mode," *Automatica*, vol. 41, no. 11, pp. 1957–1964, 2005.

[15] M. Galicki, "Finite-time control of robotic manipulators," *Automatica*, vol. 51, pp. 49–54, 2015.

[16] V. Utkin, J. Guldner, and J. Shi, *Sliding Mode Control in Electro-Mechanical Systems*. Boca Raton, FL, USA: CRC Press, 2009.

[17] C. Edwards and S. Spurgeon, *Sliding Mode Control: Theory and Applications*. Boca Raton, FL, USA: CRC Press, 1998.

[18] A. Levant, "Sliding order and sliding accuracy in sliding mode control," *Int. J. Control*, vol. 58, no. 6, pp. 1247–1263, 1993.

[19] V. Utkin and H. Lee, "Chattering problem in sliding mode control systems," in *Proc. IEEE Int. Variable Struct. Syst. (VSS'06)*, 2006, pp. 346–350.

[20] C. J. Fallaha, M. Saad, H. Y. Kanaan, and K. Al-Haddad, "Sliding-mode robot control with exponential reaching law," *IEEE Trans. Ind. Electron.*, vol. 58, no. 2, pp. 600–610, Feb. 2011.

[21] O. Barambones and P. Alkorta, "Position control of the induction motor using an adaptive sliding-mode controller and observers," *IEEE Trans. Ind. Electron.*, vol. 61, no. 12, pp. 6556–6565, Dec. 2014.

[22] H. Lee and V. I. Utkin, "Chattering suppression methods in sliding mode control systems," *Annu. Rev. Control*, vol. 31, no. 2, pp. 179–188, 2007.

[23] M.-L. Tseng and M.-S. Chen, "Chattering reduction of sliding mode control by low-pass filtering the control signal," *Asian J. Control*, vol. 12, no. 3, pp. 392–398, 2010.

[24] S. Di Gennaro, J. Rivera Dominguez, and M. A. Meza, "Sensorless high order sliding mode control of induction motors with core loss," *IEEE Trans. Ind. Electron.*, vol. 61, no. 6, pp. 2678–2689, Jun. 2014.

[25] A. Levant, "Principles of 2-sliding mode design," *Automatica*, vol. 43, no. 4, pp. 576–586, 2007.

[26] Y.-J. Huang, T.-C. Kuo, and S.-H. Chang, "Adaptive sliding-mode control for nonlinear systems with uncertain parameters," *IEEE Trans. Syst. Man Cybern. B, Cybern.*, vol. 38, no. 2, pp. 534–539, Apr. 2008.

[27] F. Plestan, Y. Shtessel, V. Bregeault, and A. Poznyak, "Sliding mode control with gain adaptation—Application to an electropneumatic actuator," *Control Eng. Pract.*, vol. 21, no. 5, pp. 679–688, 2013.

[28] M. Zhihong, M. O'day, and X. Yu, "A robust adaptive terminal sliding mode control for rigid robotic manipulators," *J. Intell. Robot. Syst.*, vol. 24, no. 1, pp. 23–41, 1999.

[29] M. B. R. Neila and D. Tarak, "Adaptive terminal sliding mode control for rigid robotic manipulators," *Int. J. Autom. Comput.*, vol. 8, no. 2, pp. 215–220, 2011.

[30] A. T. Azar and Q. Zhu, *Advances and Applications in Sliding Mode Control Systems*. New York, NY, USA: Springer, 2015.

[31] K. Youcef-Toumi and O. Ito, "A time delay controller for systems with unknown dynamics," *Trans. ASME, J. Dyn. Syst. Meas. Control*, vol. 112, no. 1, pp. 133–142, 1990.

[32] T. S. Hsia et al., "Robust independent joint controller design for industrial robot manipulators," *IEEE Trans. Ind. Electron.*, vol. 38, no. 1, pp. 21–25, Feb. 1991.

[33] M. Jin and P. H. Chang, "Simple robust technique using time delay estimation for the control and synchronization of Lorenz systems," *Chaos Solitons Fractals*, vol. 41, no. 5, pp. 2672–2680, 2009.

[34] M. Jin, Y. Jin, P. H. Chang, and C. Choi, "High-accuracy tracking control of robot manipulators using time delay estimation and terminal sliding mode," *Int. J. Adv. Robot. Syst.*, vol. 8, no. 4, pp. 65–78, 2011.

[35] Y.-X. Wang, D.-H. Yu, and Y.-B. Kim, "Robust time-delay control for the DC–DC boost converter," *IEEE Trans. Ind. Electron.*, vol. 61, no. 9, pp. 4829–4837, Sep. 2014.

[36] M. Jin, J. Lee, and K. K. Ahn, "Continuous nonsingular terminal sliding-mode control of shape memory alloy actuators using time delay estimation," *IEEE/ASME Trans. Mechatronics*, vol. 20, no. 2, pp. 899–909, Apr. 2015.

[37] M. Jin, J. Lee, P. H. Chang, and C. Choi, "Practical nonsingular terminal sliding-mode control of robot manipulators for high-accuracy tracking control," *IEEE Trans. Ind. Electron.*, vol. 56, no. 9, pp. 3593–3601, Sep. 2009.

[38] S. Jung and T. Hsia, "Neural network impedance force control of robot manipulator," *IEEE Trans. Ind. Electron.*, vol. 45, no. 3, pp. 451–461, Jun. 1998.

[39] S.-j. Cho, M. Jin, T.-Y. Kuc, and J. S. Lee, "Control and synchronization of chaos systems using time-delay estimation and supervising switching control," *Nonlinear Dynam.*, vol. 75, no. 3, pp. 549–560, 2014.

[40] G. R. Cho, P. H. Chang, S. H. Park, and M. Jin, "Robust tracking under nonlinear friction using time-delay control with internal model," *IEEE Trans. Control Syst. Tech.*, vol. 17, no. 6, pp. 1406–1414, Nov. 2009.

[41] K. M. Hangos, J. Bokor, and G. Szederkényi, *Analysis and Control of Nonlinear Process Systems*. New York, NY, USA: Springer, 2006.

[42] J. J. Craig, *Introduction to Robotics: Mechanics and Control*. Upper Saddle River, NJ, USA: Pearson Prentice-Hall, 2005.

[43] J.-J. E. Slotine et al., *Applied Nonlinear Control*. Englewood Cliffs, NJ, USA: Prentice-Hall, 1991.

Maolin Jin (S'06–M'08) received the B.S. degree in material science and mechanical engineering from Yanbian University of Science and Technology, Jilin, China, in 1999, and the M.S. and Ph.D. degrees in mechanical engineering from Korea Advanced Institute of Science and Technology (KAIST), Daejeon, Korea, in 2004 and 2008, respectively.

In 2008, he was a Postdoctoral Researcher with the Mechanical Engineering Research Institute, KAIST. He is currently a Senior Researcher with the Research Institute of Industrial Science and Technology, Pohang, Korea. His research interests include robust control of nonlinear plants, time-delay control, robot motion control, electro-hydraulic actuators, winding machines, and factory automation.

Dr. Jin is a member of the Institute of Control, Robotics and Systems in Korea.

Jaemin Baek (S'16) received the B.S. degree in mechanical engineering from Korea University, Seoul, Korea, in 2011. He is currently working toward the Ph.D. degree (M.S.–Ph.D. joint program) in creative IT engineering (CiTE) at Pohang University of Science and Technology (POSTECH), Pohang, Korea.

His research interests include high-accuracy positioning applications, controller design for industrial systems, robust control of nonlinear systems, and time-delay control.

Soohee Han (M'12–SM'13) received the B.S. degree in electrical engineering in 1998 and the M.S. and Ph.D. degrees in electrical engineering and computer science in 2000 and 2003, respectively, from Seoul National University (SNU), Seoul, Korea.

From 2003 to 2007, he was a Researcher with the Engineering Research Center for Advanced Control and Instrumentation, SNU. In 2008, he was a Senior Researcher with the Robot S/W Research Center, Seoul, Korea. From 2009 to 2014, he was with the Department of Electrical Engineering, Konkuk University, Seoul, Korea. Since 2014, he has been with the Department of Creative IT Engineering, Pohang University of Science and Technology (POSTECH), Pohang, Korea. His research interests include computer-aided control system designs, distributed control systems, time-delay systems, and stochastic signal processing.